Advances in Aircraft and Spacecraft Science, *Vol. 3, No. 1 (2016) 77-93*
DOI: http://dx.doi.org/10.12989/aas.2016.3.1.077

Gasdynamics of rapid and explosive decompressions of pressurized aircraft including active venting

Alfonso Pagani* and Erasmo Carrera[a]

Department of Mechanical and Aerospace Engineering, Politecnico di Torino
Corso Duca degli Abruzzi 24, 10129 Torino, Italy

(Received July 6, 2015, Revised July 24, 2015, Accepted August 3, 2015)

Abstract. In this paper, a zero-dimensional mathematical formulation for rapid and explosive decompression analyses of pressurized aircraft is developed. Air flows between two compartments and between the damaged compartment and external ambient are modeled by assuming an adiabatic, reversible transformation. Both supercritical and subcritical decompressions are considered, and the attention focuses on intercompartment venting systems. In particular, passive and active vents are addressed, and mathematical models of both swinging and translational blowout panels are provided. A numerical procedure based on an explicit Euler integration scheme is also discussed for multi-compartment aircraft analysis. Various numerical solutions are presented, which highlight the importance of considering the opening dynamics of blowout panels. The comparisons with the results from the literature demonstrate the validity of the proposed methodology, which can be also applied, with no lack of accuracy, to the decompression analysis of spacecraft.

Keywords: rapid decompression; explosive decompression; isentropic model; active venting; blowout panels

1. Introduction

In order to provide fast transfers and efficient flights, from the beginning of the second half of the 20th century, public air transport operates at a high altitude of approximately 12000 meters. Operational altitudes continue to remain consistent, even in modern times (apart from some special cases, i.e., supersonic aircraft). The effects on people of exposure to those high altitudes have been extensively studied; see for example (Garner 1999, Roth 1968). In these studies, researchers clearly demonstrated that significant human performance losses ranging from impairment to death start approximately at altitudes beyond 3000 m. For this reason, according to CS-25 regulations (EASA 2014), pressurized compartments to be occupied must be equipped to provide a cabin pressure altitude of no more than 2438 m at the maximum operating altitude of the aircraft under normal operating conditions.

Although pressurized fuselage protects crew and passengers from the lethal environmental

*Corresponding author, Research Fellow, E-mail: alfonso.pagani@polito.it
[a]Professor, E-mail: erasmo.carrera@polito.it

Copyright © 2016 Techno-Press, Ltd.
http://www.techno-press.org/?journal=aas&subpage=7 ISSN: 2287-528X (Print), 2287-5271 (Online)

effects, decompression accidents continue to be the cause of aircraft and lives losses. Fuselage decompression can result from several events, such as structural failure, puncturing by broken turbine blades, malfunction of the pressurization system, and loss of a window. Decompression phenomena are categorized into explosive, rapid and slow. In this work, we are mainly interested in explosive and rapid decompression. The former takes tenths of a second for the pressure loss to occur. On the other hand, rapid decompression are defined in terms of seconds.

One of the most famous accident caused by a decompression event is the one that interested the Aloha Airlines Flight 243 between Hilo and Honolulu in Hawaii (NTSB 1989). On April 28, 1988, a Boeing 737-297 serving the flight was subjected to an explosive decompression that caused severe damage and the loss of a section of the upper fuselage. The aircraft, however, was able to land safely at Kahului Airport on Maui, but one flight attendant was swept overboard from the airplane and another 65 passengers and crew were injured, mainly from flying debris. During decompression, in fact, the air mass moves through the aircraft compartments in a non-uniform manner and this cause pressure differentials that may further damage primary and secondary structures. For this reason, according to CS-25 regulations (EASA 2014), civil aircraft must be designed to withstand loads from rapid decompressions and not only the normal operational loads.

It is, therefore, clear that the interest in developing accurate models for the calculation of pressure changes within the compartments of a pressurized aircraft is of great interest still today. One of the pioneering work in rapid decompression analysis is the report by Haber and Clamann (1953). They clearly analyzed the complexity of the phenomenon and developed a zero-dimensional polytropic model for the analysis of a punctured chamber. They also performed experimental measurements using small chambers, and they revealed that a polytropic transformation with an exponent of n=1.16 well describes the decompression event. They provided practical formulae for evaluating decompression times in both supercritical and subcritical regions, and the chamber volume change was also taken into consideration. However, their report focused on the analysis of a single pressurized chamber. Demetriades (1954) developed an isentropic model for the analysis of punctured spacecraft in vacuum flight. He estimated the decompression time as a function the initial and final pressures. However, he did not consider any repressurization, which is the most common countermeasure to decompression in modern spacecraft. Mavriplis (1963) published a comprehensive paper about rapid decompression of aircraft and spacecraft. He developed isothermal, isentropic and polytropic models for punctured pressurized chambers and provided various numerical examples about single, two- and three-compartment cabins. He formulated equations for the calculation of air outflow, decompression time, required air inflow to the cabin to increase decompression time, and pressure-time histories of the individual compartment. In a very recent work, Burlutskiy (2012) investigated rapid decompression of multi-component gas mixture flows in pipes via a one-dimensional model. Some conclusions outlined in his work would find interesting exploitation in aerospace applications.

In the works mentioned above, the authors did not consider intercompartment active venting. Active vents are panels that timely open as a design pressure differential between two compartments is reached. These devices allow to facilitate the flow of air and the re-equalization of pressure, thus limiting pressure forces on the structures. Pratt (2006) recently modeled swinging and translational blowout panels in the analysis of aircraft decompression. He developed an isentropic model and highlighted the importance of considering panels weight in the estimation of pressure differentials between compartments. However, in his paper he only considered subcritical decompressions, which can be of interest for operational altitudes lower than approximately 7300 m. Daidzic and Simones (2010) developed zero-dimensional isothermal and isentropic models of

cockpit and cabin decompression with cockpit security door. In their study, two hinged panels in the security door were modeled to account for the pressure equalization dynamics in the case of both cockpit and cabin decompressions. In their work, various analytical solutions were provided along with formulae for decompression time evaluation. However, passive and active venting systems enabling communication among compartments were assumed to be instantaneous and only single- and two-compartment systems were analyzed.

In the present work, the attention is mainly focused on the modelling of active vents within an isentropic model for aircraft and spacecraft decompression. First, the theoretical modelling of the phenomenon is briefly introduced for both subcritical and supercritical flows. The models of both hinged and translational blowout panels including inertial effects are then discussed in Section 3. A general numerical procedure is subsequently devised for the solution of the coupled differential equations for arbitrary multi-compartment aircraft. Next, numerical results are provided in Section 5, where single- to four-compartment cabins are addressed and the importance to consider the dynamics of active venting systems is discussed. The main conclusions are finally outlined in Section 6.

2. Theoretical framework

In this work, a simple zero-dimensional model is presented and used to evaluate the pressure, density and temperature changes within a pressurized fuselage undergoing a decompression event. As discussed by Haber and Clamann (1953), decompression is a very complex phenomenon, involving heat transfer, irreversible effects and phase changes. Haber (1950) measured that temperature drop associated with rapid decompression can be around 100°C. Therefore, to treat the process as an isothermal one is not justified. Moreover, because of heat exchange between air and aircraft walls, the assumption of adiabatic transformation is not justified as well. Haber (1950) also demonstrated that, because the temperature drops below the dew point in the first instants of the decompression, the effects of humidity could not be neglected. Thus, decompression should be treated as a polytropic process.

However, as demonstrated by Daidzic and Simones (2010), an adiabatic, reversible (isentropic) process can be assumed with acceptable accuracy in the case of explosive (within 0.5 s) and rapid (within 10 s) decompressions. The following hypotheses are also adopted in the present formulation:

- the fuselage volume does not change during the decompression;
- the external atmosphere is considered as an infinite volume that does not change as a consequence of the fuselage outflow;
- diabatic and irreversible effects through venting areas and breaches are taken into account by adopting a discharge coefficient, C_D;
- air is considered as an ideal gas;
- the outside pressure fluctuations along the fuselage are not taken into account in this study. Nevertheless, this effect might be included with no difficulties by considering an equivalent average flight level or appropriate pressure coefficients that come from aerodynamic analyses.

2.1 Isentropic model of the fuselage decompression

A fuselage composed by a certain number of compartments is considered. The compartments

can communicate each other by passive or active vents. The former are considered always open and no special considerations are needed. The latter will be discussed in the next section. The variation of the mass of gas within the i-th compartment, m_i, is described by the mass conservation equation, whose differential form holds

$$\frac{dm_i}{dt} = \dot{m}_{in} - \dot{m}_{out} \tag{1}$$

where $\dot{m}_{in} - \dot{m}_{out}$ is the net flux of the mass flow rate. In particular, $\dot{m}_{in}$ is the sum of the mass inflows that come into compartment i either from the communicating chambers or from a repressurization security system; and $\dot{m}_{out}$ is the sum of the mass outflows that exit chamber i either through the fuselage breach (if i is the damaged compartment) or through the vents towards communicating chambers.

In general, the mass flow rate from a chamber i towards a chamber j ($p_i > p_j$) depends, of course, on the pressure ratio between the two compartments. The flow through the vent connecting the two compartments can be either sonic ($M = 1$, critical/superctitical or choked flow) or subsonic ($M < 1$, subcritical flow). Given the pressure of chamber j, p_j, the critical pressure of chamber i, p_i^*, such that the flow is supercritical is (Streeter 1975)

$$\frac{p_i^*}{p_j} = \left(\frac{\gamma + 1}{\gamma}\right)^{\frac{\gamma}{\gamma-1}} \tag{2}$$

In the case of isentropic transformation, the specific heat ratio γ is equal to 1.4, thus

$$p_i^* = 1.893\, p_j \tag{3}$$

By assuming the vent as a quasi-1D duct, when the compartment pressure p_i is greater or equal to p_i^*, the flow in correspondence of the vent throat is sonic and the outflow mass rate is the maximum possible. In this case, the mass flow rate from compartment i to compartment j only depends on the thermodynamic state of compartment i and not on the state of the downstream compartment.

$$\dot{m}_{ij}^* = \rho_i \left(\frac{2}{\gamma + 1}\right)^{\frac{1}{\gamma-1}} A_{eff} \sqrt{\frac{2\gamma R T_i}{\gamma + 1}} \tag{4}$$

where ρ_i and T_i are, respectively, the density and temperature of chamber i; $R = 287\, J/kg\, K$ is the ideal gas constant; and A_{eff} is the effective area of the vent and it is calculated by multiplying the actual area A with the discharge coefficient $C_D < 1$ for taking into account irreversible phenomena. In fact, C_D represents the ratio between the actual diabatic flow rate and the approximate isentropic flow rate (Holman 1980). The discharge coefficient can be evaluated trough measurements, complex CFD analyses (Bréard *et al.* 2004) or via sensitivity analyses (Daidzic and Simones 2010). In the case in which $p_i < p_i^*$, the mass flow rate will depend on the conditions of both chambers i and j; i.e.

$$\dot{m}_{ij} = A_{eff} \sqrt{2 p_i \rho_j \frac{\gamma}{\gamma - 1} \left(\frac{p_j}{p_i}\right)^{\frac{2}{\gamma}} \left[1 - \left(\frac{p_j}{p_i}\right)^{\frac{\gamma-1}{\gamma}}\right]} \tag{5}$$

Eqs. (4) and (5) can also be used to evaluate the outflow mass rate from the damaged compartment to the ambient. One has only to opportunely substitute the proper thermodynamic quantities in the equations above. It should also be underlined that one cannot exclude a priori the possibility that sonic flow exists between two aircraft compartments. This situation can, in fact, be possible in the case of active venting with sufficiently high release pressure of the blowout panels (see Section 3).

Under the hypothesis of constant compartment volume, it is straightforward to relate the density change to the net flux of the mass flow rate. In fact,

$$\frac{dm_i}{dt} = \frac{d}{dt}(\rho_i V_i) = V_i \frac{d\rho_i}{dt} \tag{6}$$

where V_i is the volume of the i-th chamber. By substituting Eq. (6) into Eq. (1), one has

$$\frac{d\rho_i}{dt} = \frac{1}{V_i}(\dot{m}_{in} - \dot{m}_{out}) \tag{7}$$

It is clear that, given an aircraft made of N compartments, Eq. (7) can be used for each chamber resulting into a system of N coupled differential relations in $3 \times N$ unknowns, i.e., pressure, density and temperature changes in each compartment. The problem can be solved by adding to the system described by Eq. (7) the perfect gas law (equation of state), which actually has already been implicitly used, and the isentropic transformation relations.

Isentropic processes are regulated by well-known relations (Streeter 1975) that, for example, can be used to correlate the thermodynamic quantities of chamber i at the generic time t with the same quantities at the initial state, namely p_c^0, ρ_c^0, and T_c^0:

$$\frac{T_i}{T_c^0} = \left(\frac{p_i}{p_c^0}\right)^{\frac{\gamma-1}{\gamma}} = \left(\frac{\rho_i}{\rho_c^0}\right)^{\gamma-1} \tag{8}$$

3. Active venting

In order to minimize the risks due to rapid decompression, passive and active venting between compartments are usually used in modern pressurized aircraft (Langley 1971, Pratt 2006). The aim of those vents, in fact, is to provide sufficiently fast air discharge to timely avoid pressure picks on primary and secondary structures during a decompression.

Passive venting enabling communication between compartments are considered always open. On the other hand, the area of an active vent is considered null until a certain pressure differential between the chambers is reached. Assuming the opening of active vents as instantaneous may result in an underestimation of the structural loads (Pratt 2006). Thus, a proper simulation of the dynamics of the blowout panels is necessary. Of course, the opening of the active venting area depends on the type of blowout panel adopted. In this paper, two different types of blowout panels are considered. Namely, hinged panels and translational panels.

3.1 Hinged blowout panels

A simple hinged panel connecting two compartments at different pressures is shown in Fig. 1. The dynamics of hinged panels and door are regulated by the second Newton law, in the form

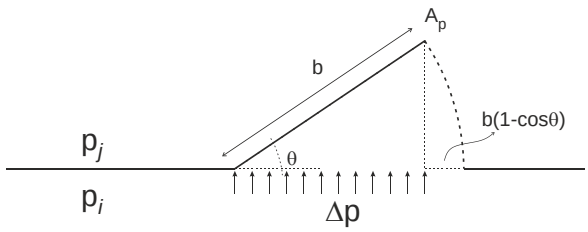

Fig. 1 Hinged blowout panel

$$\sum M = \frac{d^2\theta}{dt^2} I \tag{9}$$

where $\sum M$ is the summation of the moments acting on the blowout panel, θ is the rotation angle with respect to the fixed rotation point, and I is the moment of inertia of the panel. In the present paper, the only moment acting on the panel is considered to be the moment due to the differential pressure $\Delta p = p_i - p_j$; i.e.

$$\sum M = \Delta p\, A_p\, cos\theta\, \frac{b}{2}\, cos\theta = \frac{1}{2}\Delta p\, A_p\, b\, cos^2\theta \tag{10}$$

where $A_p cos\theta$ is the projection of the panel area on the closed configuration plane, and b is the dimension of the panel along a direction perpendicular to the rotation axis. Other effects might be included into Eq. (10), such as friction and panel weight.

It is easy to verify that the moment of inertia of the panel with respect ot the rotation axis is

$$I = \frac{m_p b^2}{3} \tag{11}$$

where m_p is the mass of the blowout panel. By substituting Eqs. (10) and (11) into Eq. (9), the differential equation regulating the variation of the panel rotation angle is obtained.

$$\frac{d^2\theta}{dt^2} = \frac{3\Delta p A_p\, cos^2\theta}{2 m_p b} \tag{12}$$

the initial conditions being $\theta(0) = 0$, $\frac{d\theta}{dt}(0) = 0$. Equation (12) is valid for $\Delta p > p_{rel}$, where p_{rel} is the pressure required to overcome the detent torque and starting opening the hinged panel. As long as $\Delta p < p_{rel}$, the panel remains closed.

The open area between two compartments that are separated by a rotational blowout panel is a function of the rotation angle θ. For example

$$A_{open} = A_p(1 - cos\theta) \tag{13}$$

In principle, also the dischange coefficient related to the blowout panel may be considered as a function of θ, see for example the work by Daidzic and Simones (2010). However, it is clear that it is not easy to quantify this effect, which is therefore not considered in the present work.

3.2 Translational blowout panels

As shown in Fig. 2, a translational blowout panel is a device that, ideally, timely detach on all

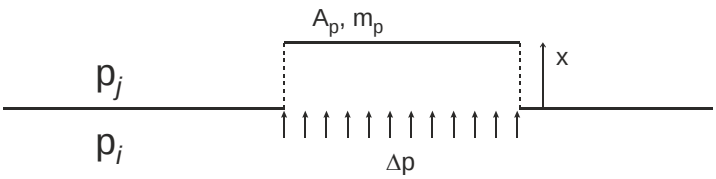

Fig. 2 Translational blowout panel

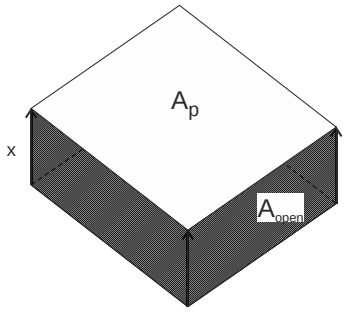

Fig. 3 Area swept by a translational panel during detachment

its sides as the pressure differential between two compartments is equal to the release pressure p_{rel}. The motion of the translational blowout panel is described by the second Newton law, in the form

$$\sum F = \frac{\partial^2 x}{\partial t^2} m_p \tag{14}$$

where $\sum F$ is the summation of the forces acting on the panel and x is the displacement from the rest position. In this paper, only the forces due to the differential pressure between the chambers is considered, which is of course $\sum F = \Delta p\, A_p$. Thus, the differential equation regulating the variation of the panel movement is

$$\frac{\partial^2 x}{\partial t^2} = \frac{\Delta p\, A_p}{m_p} \tag{15}$$

the initial conditions being $x(0) = 0$, $\frac{dx}{dt}(0) = 0$. Eq. (15) is valid for $\Delta p > p_{rel}$, where p_{rel} is the pressure required to overcome the detent force and starting opening the translational panel. As long as $\Delta p < p_{rel}$, the panel remains closed.

The open area between two compartments that are separated by a translational blowout panel is a function of the displacement x. For example, with reference to Fig. 3, one may consider the open area as the minimum quantity between the actual panel area and the area swept by the panel during the detachment. In formula

$$A_{open} = min\left[2\left(\frac{A_p}{b} + b\right)x,\ A_p\right] \tag{16}$$

where b is the dimension of one of the sides of the panel.

It should be mentioned that translational panels might hurt passengers and crew during a decompression event. For this reason they are usually secured by lanyards.

4. Numerical solution procedure

The analysis of an aircraft made of N compartments, according to the models discussed in the previous sections, would result in the resolution of a system of $(N + N_h + N_t)$ nonlinear, coupled, ordinary differential equations (ODEs), N_h being the number of hinged blowout panels and N_t the number of translational blowout panels. In this paper, an explicit Euler integration scheme is adopted and it is briefly discussed hereafter.

The analysis time is discretized into a number of steps; i.e., $t_{in} = t_1 < t_2 < t_3 < \cdots < t_k < \cdots < t_n = t_{fin}$, where t_{in} is the initial starting time and t_{fin} is the final time. Presumably, $t_{in} = 0$ is the time in which the fuselage breach/puncture appears. The breach generation is assumed instantaneous in this work. At $t = t_{in}$ all the aircraft compartments are assumed to be at the initial state p_c^0, ρ_c^0, T_c^0. At the generic time step t_{k+1}, the density within the i-th chamber, ρ_{k+1}, can be calculated by directly integrating Eq. (7). It reads

$$\rho_{k+1} = \rho_k + \frac{1}{V_i} m'_k \Delta t \tag{17}$$

where ρ_k is the density of chamber i at time t_k; V_i is the volume of chamber i and it is constant; Δt is the time step interval; and m'_k is the derivative with respect to time of the mass of gas in the chamber at time t_k. m'_k is calculated according to Eq. (1), i.e. by evaluating the net flux of the mass flow rates within the chamber under consideration at time t_k according to Eqs. (4) and (5). It is clear that, when $k = 1$ (i.e., $t_k = t_{in}$), m'_k in non-null only in the damaged compartment.

In evaluating the mass variation at time t_k within the compartment, the proper active areas should be considered in Eqs. (4) and (5). For doing this, depending on the type of active vents, Eqs. (12) and (15) must be integrated. Let us consider the case of a hinged blowout panel. We consider θ_k as the approximation of $\theta(t)$ at time t_k. Similarly, v_k is the approximation of $\theta'(t)$ at time t_k. The second-order ODE in Eq. (12) can be divided into two first-order ODEs by introducing the new variable v_k. θ_k is therefore given by (for $k > 1$)

$$\begin{aligned} \theta_k &= \theta_{k-1} + v_{k-1}\Delta t \\ v_k &= v_{k-1} + \frac{3\Delta p_{k-1} A_p \cos^2\theta_{k-1}}{2 m_p b}\Delta t \end{aligned} \tag{18}$$

Eq. (15) can be integrated in a similar manner. Once the rotations and displacements of the blowout panels at time t_k are known, the related open areas can be calculated through Eqs. (13) and (16). It should be underlined that a time step interval $\Delta t = 50\ \mu s$ was sufficient for providing accurate and convergent solutions for all the cases considered, see also (Pratt 2006).

Once the density ρ_{k+1} (Eq. (17)) in each compartment is calculated, the related pressure p_{k+1} and temperature T_{k+1} are evaluated by the isentropic relations of Eq. (8).

5. Results

5.1 Single-chamber decompression

In the first analysis case, the decompression of a single chamber is considered. The chamber

Table 1 Decompression times of the single chamber

	Supercritical phase duration	Subcritical phase duration	Total decompression time
	$\frac{t_{sup}}{V/A} \times 10^3 \left(\frac{s}{m}\right)$	$\frac{t_{sub}}{V/A} \times 10^3 \left(\frac{s}{m}\right)$	$\frac{t_{tot}}{V/A} \times 10^3 \left(\frac{s}{m}\right)$
Present model	3.23	3.82	7.05
Daidzic and Simones (2010)	3.23	3.95	7.18
Haber and Clamann (1953)	4.43	4.09	8.52

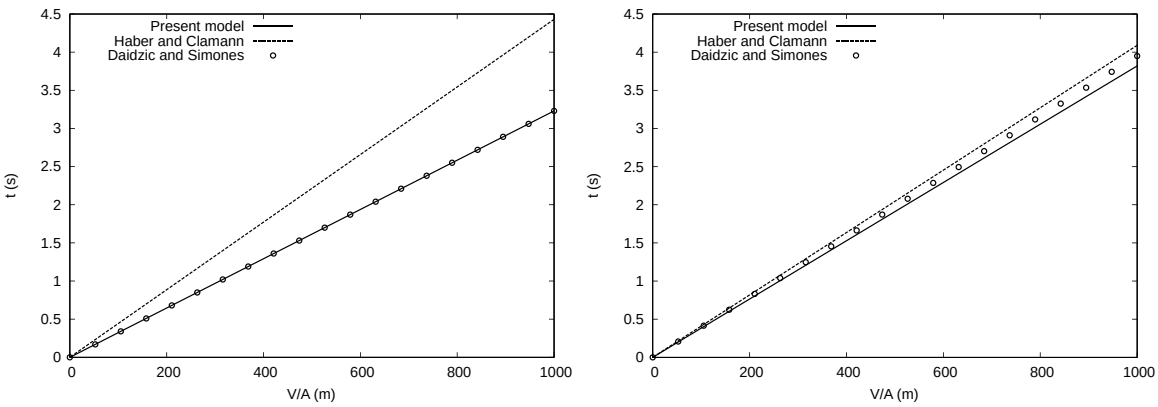

(a) Supercritical outflow (b) Subcritical outflow

Fig. 4 Supercritical and subcritical phases durations of the single chamber for various V/A ratios

has a volume equal to $4\ \mathrm{m}^3$. The initial internal pressure and temperature are $p_c^0 = 117.013$ kPa and $T_c^0 = 23°\mathrm{C}$, respectively. The ambient pressure is $p_a = 26.4289$ kPa, whereas the ambient external temperature is $T_a = -50°\mathrm{C}$. A sudden breach with effective area equal to A is simulated.

In Table 1 the supercritical and subcritical phase durations as well as the total decompression time according to the present numerical model are compared to reference solutions from the literature, namely (Haber and Clamann 1953, Daidzic and Simones 2010). In the table, decompression times are given as functions of the ratio between cabin volume and breach effective area. Haber and Clamann (1953) provided decompressions times by using a polytropic model and separate diagrams. Daidzic and Simones (2010) formulated practical analytical formulae for decompression time evaluations by using an isentropic model, which is equivalent to the present one. Subcritical and supercritical phase durations are also given in graphical form in Fig. 4 as functions of V/A.

It is clear that the difference between an isentropic model and a polytropic one is mainly visible in the duration of the supercritical decompression phase (Fig. 4(a)). For the particular case under consideration, the difference between the isentropic models and the polytropic one is approximately equal to 27%. Although, the isentropic transformation is for sure more accurate for explosive events. For higher decompression durations, a polytropic transformation should be used. However, the error committed by the isentropic model in this case could be reduced by opportunely tuning the discharge coefficient C_D for the effective area calculation. Nevertheless,

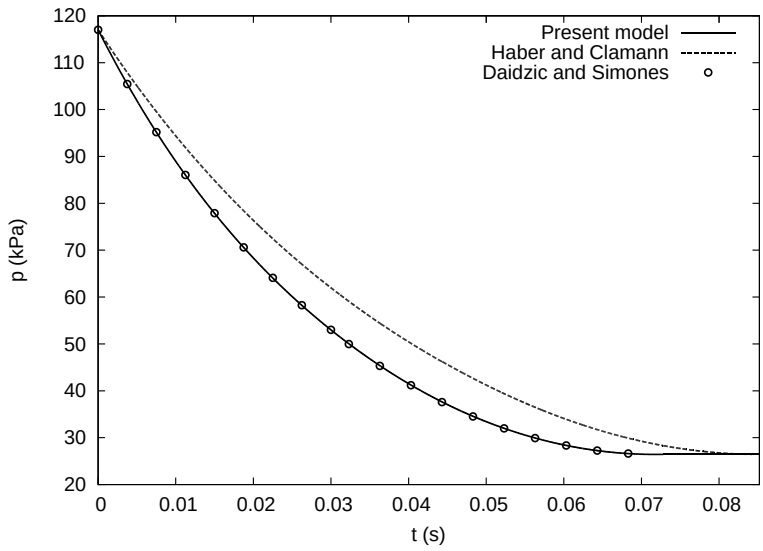

Fig. 5 Pressure history within the single chamber for *V/A*=10 m

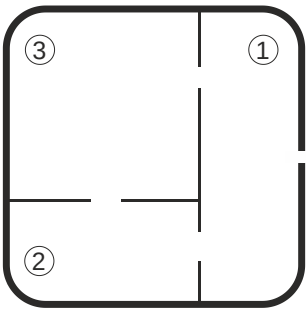

Fig. 6 Three-compartment cabin as in (Mavriplis 1963)

the analysis clearly shows the good agreement between the analytical solution provided by Daidzic and Simones (2010) and the present numerical model. The small difference in the subcritical phase duration is mainly due to the fact that Daidzic and Simones (2010) calculated the supercritical/subcritical phases change as well as the total discharge time by using an analytical (approximate) formula, whereas in the present study the phase change and decompression times are calculated by comparing pressure ratios at each time step.

For the sake of completeness, the time-history pressure loss within the chamber for $V/A = 10$ m and various decompression models is shown in Fig. 5.

5.2 Three-compartment cabin

In order to verify the capability of the proposed methodology to deal with multi-compartment aircraft, the cabin shown in Fig. 6 is analyzed for further verification. The same problem was addressed by Mavriplis (1963). The aircraft is considered to fly at 9144 m (30000 ft), when it experiences failure of the cockpit window (compartment 1). The cabin, which is pressurized with an initial differential pressure equal to $(p_c^0 - p_a) = 48.608$ kPa (7.05 psi), is divided into three

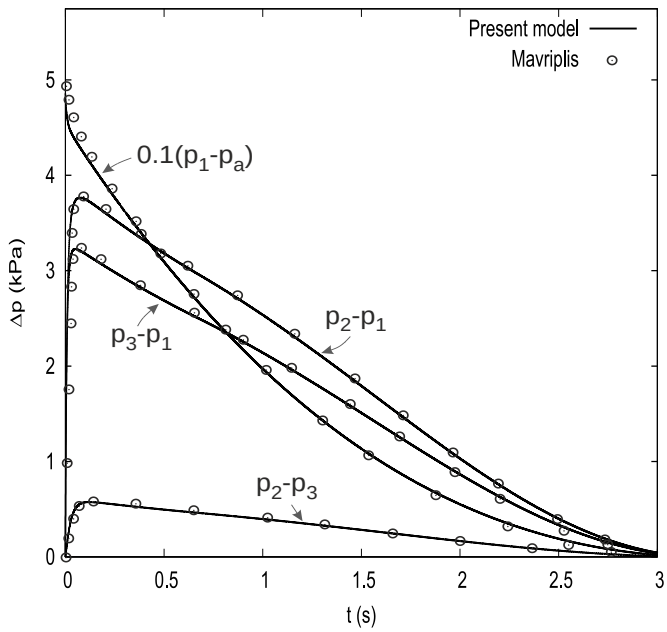

Fig. 7 Decompression of the three-compartment cabin

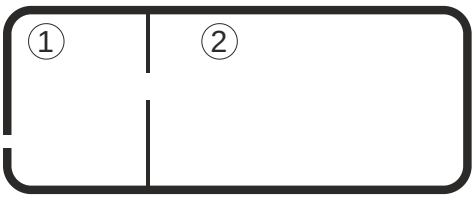

Fig. 8 Two-compartment aircraft with active venting between compartments 1 and 2

compartments, i.e., cockpit $V_1 = 14.72$ m^3 (520 ft^3), cargo $V_2 = 98.68$ m^3 (3485 ft^3), and passengers cabin $V_3 = 207.90$ m^3 (7342 ft^3). An instantaneous and complete loss of the window, whose total effective area is $A_{1a} = 0.511$ m^2 (5.5 ft^2), is assumed. Passive vents between each couple of compartments are considered as in Fig. 6. The effective venting areas are as follows: $A_{21} = 0.019$ m^2 (0.2 ft^2), $A_{23} = 0.789$ m^2 (8.5 ft^2), and $A_{31} = 1.115$ m^2 (12 ft^2).

Fig. 7 shows the differential pressure values between each compartment and cockpit and ambient. The results show a very good correspondence between the present model and the isentropic model by Mavriplis (1963), who solved the coupled system of ODEs by using a Runge-Kutta direct integration method. In this example, equalization of pressure is achieved within 3.16 s, of which the first 0.79 s are interested by sonic flow in the breach throat. The maximum pressure differential is experienced between the cockpit and the passengers cabin, and it is equal to 3.77 kPa. This pick is measured approximately at a time equal to 0.073 s from the window loss.

5.3 Two-compartment aircraft with active venting

In this example, the dynamics of the active vents discussed in Section 4 are demonstrated by using a simple two-compartment cabin as in Fig. 8. In this example, the net cockpit volume is

$V_1 = 4$ m^3, whereas the cabin has a volume equal to $V_2 = 60$ m^3. The initial conditions of the aircraft are $p_c^0 = 78.959$ kPa and $T_c^0 = 23$°C. The aircraft is flying at an altitude such that the external temperature is $T_a = -54.65$°C and the maximum ratio between cabin and ambient pressures is $p_c^0/p_a = 4$. A sudden breach with area $A = 0.5$ m^2 and $C_D = 0.8$ appears in the cockpit.

In the first analysis case, a swinging blowout panel is assumed between cabin and cockpit. The dimension of the panel along the direction perpendicular to the rotation axis is $b = 0.5$ m, whereas the effective active venting area is $AC_D = 0.25$ m^2. The weight of the panel is equal to 6.75 kg and the pressure needed to overcome the detent torque is $p_{rel} = 12$ kPa. Pressure and temperature variations within the two compartments are shown in Fig. 9. The active area opening, which is directly correlated to the panel rotation θ, is shown in Fig. 10(a). It is interesting to note that the cockpit experiences a recompression, as the blowout panel is open. The results demonstrate the severe conditions crew and passengers would face in the case of a rapid decompression. In this case, which mimic a real event, after about 1.7 s, the cabin temperature

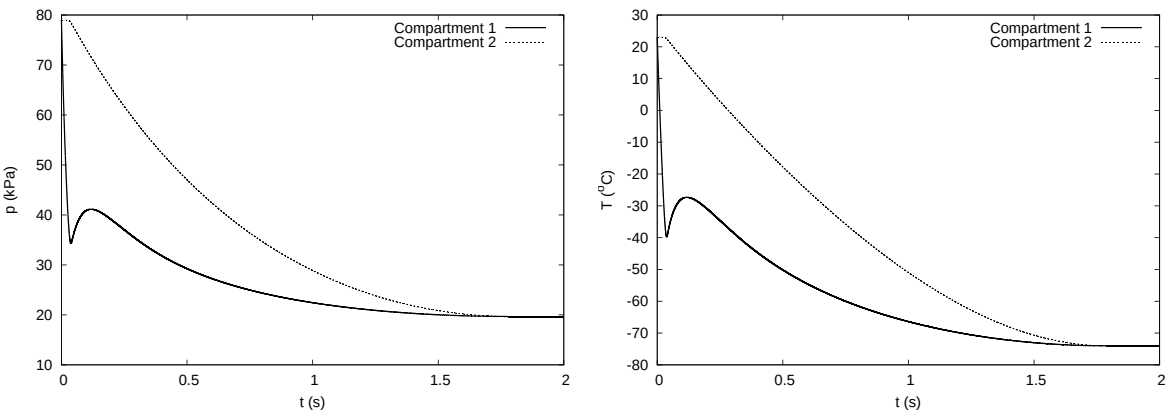

(a) Pressure variation (b) Temperature variation

Fig. 9 Decompression of the two-compartment aircraft with hinged blowout panel between compartments 1 and 2

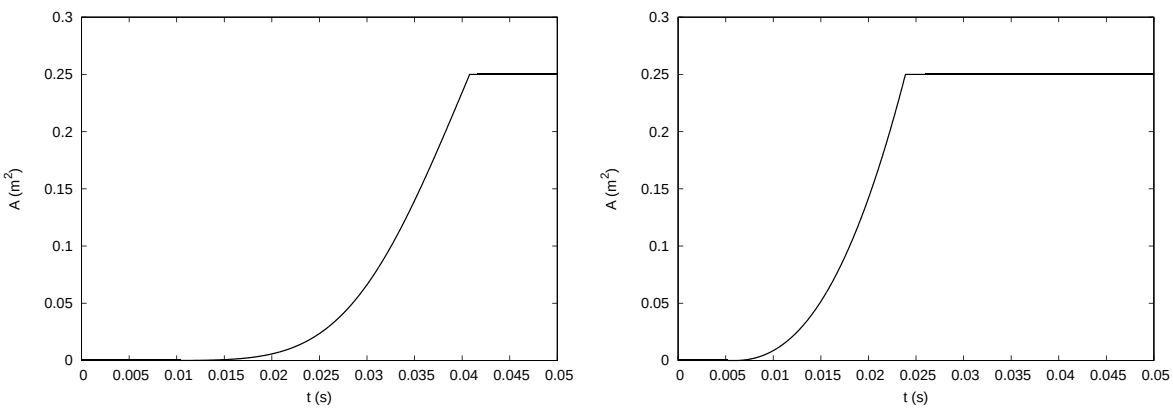

(a) Hinged panel (b) Translational panel

Fig. 10 Active area between compartments 1 and 2 versus time

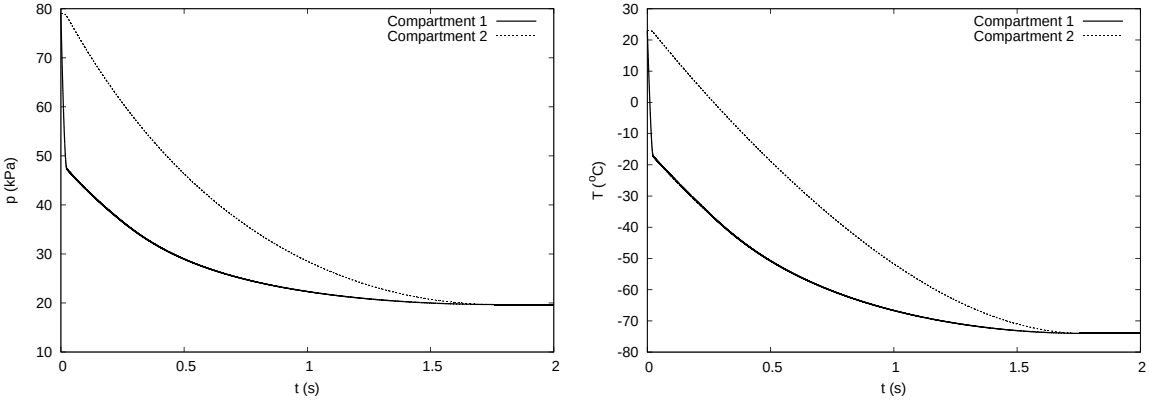

(a) Pressure variation (b) Temperature variation

Fig. 11 Decompression of the two-compartment aircraft with translational blowout panel between compartments 1 and 2

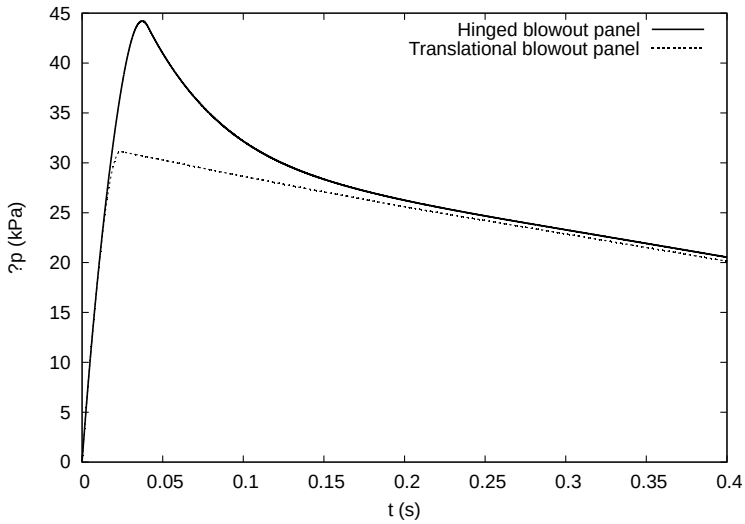

Fig. 12 Differential pressure between the compartments of the two-compartment aircraft, $(p_2 - p_1)$

drops from 23°C to −74°C. In reality, as highlighted by Daidzic and Simones (2010), the water vapour in the cabin would condense and freeze. Neglecting this effect results in the minimum air temperature possible. Moreover, the heat transfer between ambient and fuselage will equalize the temperature, that should be about T_a within the aircraft if altitude is maintained.

In the second analysis case, a translational blowout panel is considered between the two compartments. The translational panel has exactly the same characteristics as the hinged panel addressed in the previous analysis. The time history of the effective area between cockpit and cabin is shown in Fig. 10(b). From comparison with Fig. 10(a), it is clear that the translational panel opens faster than the swinging panel. As a result, as shown in Fig. 11, cockpit does not experience a recompression. Pressure and temperature variations, however, slow down as the translational panel is open, because of the additional air that flows from cabin to cockpit.

The choice of the blowout panel type also reflects on the pressure loads between the two

Table 2 Decompression of the two-compartment aircraft; comparison between hinged and translational blowout panels

	Panel opening time* (ms)	Duration of the supercritical phase (ms)	Duration of the subcritical phase (ms)	Total decompression duration	Differential pressure pick, $p_2 - p_1$ (kPa)
Hinged panel	40.8	726	1029.5	1755.5	44.21
Translational panel	23.9	712	1028.7	1740.7	31.14

*Time for reaching the maximum venting area from $t = 0$

compartments. This aspect is clarified in Fig. 12, where the differential pressure between cabin and cockpit in the first instants of the decompression event is shown. The picture clearly proves that the use of translational panel results in lower pressure loads on the intercompartment structures. In other words, the faster the active vent opens the lower pick differential pressures. Indirectly, this conclusion also highlights the importance of considering blowout panels dynamics. Considering instantaneous openings would result, in fact, in an important, non-negligible underestimation of the structural loads due to the rapid decompression event.

Table 2 further underline the previous conclusions. This table, in fact, for both the cases of hinged and translational panels, quotes the panel opening times, the decompression times, including supercritical and subcritical phases, and the maximum differential pressure between cockpit and cabin. It is clear that decompression time is slightly influenced by panel opening time. On the other hand, the maximum differential pressure in the case of swinging panel is some 30% higher than the case of the translational panel.

5.4 Four-compartment aircraft

In the final analysis case, a four-compartment aircraft as in Fig. 13 is considered. The fuselage has the cockpit with volume $V_1 = 4$ m^3, entryway $V_2 = 3$ m^3, passengers cabin $V_3 = 198$ m^3, and cargo $V_4 = 67$ m^3. The internal initial conditions of the aircraft are $p_c^0 = 89.786$ kPa and $T_c^0 = 23$°C. The aircraft is flying at 9980 m ($p_a = 26.5$ kPa, $T_a = -49.85$°C) when a rapid decompression starts. The decompression is due to a breach in the entryway (compartment 2) of area $A_{2a} = 0.6$ m^2. A discharge coefficient $C_{D_{2a}} = 0.8$ is assumed for the breach. Compartments are connected each other via passive and active venting as follows (see Fig. 13):

- Passive venting between entryway (compartment 2) and passengers cabin (compartment 3). The passage has dimensions 1.8×0.5 m.
- Hinged blowout panel between cockpit (compartment 1) and entryway (compartment 2). The panel is square with sides equal to 0.4 m. The weight of the panel is 4.32 kg, whereas the release pressure is 6 kPa.
- Translational panels between cargo (compartment 4) and all the other compartments. Each translational panel is square with sides equal to 0.3 m. The weight of each panel is 2.43 kg and the pressure release is 4 kPa.

For both passive and active vents, a discharge coefficient $C_D = 0.7$ is assumed.

The decompression under consideration requires a total time of about 3.74 s to be accomplished, of which the first 1.43 s are interested by sonic outflow from entryway to external ambient. In the first moments of the event, as shown in Fig. 13, high differential pressures between

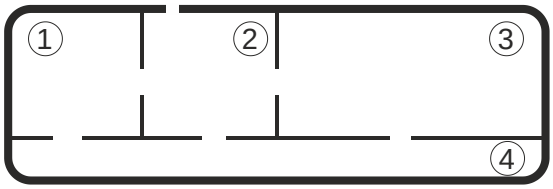

Fig. 13 Four-compartment aircraft

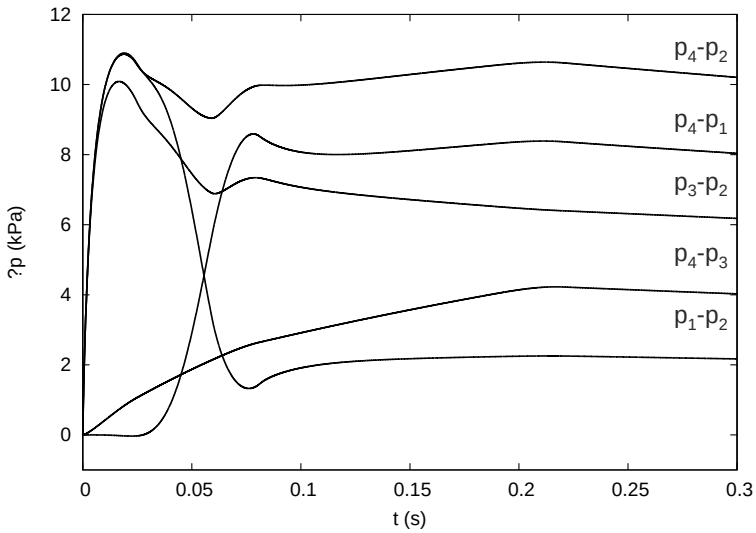

Fig. 14 Differential pressures between the compartments of the four-compartment aircraft

Table 3 Differential pressure picks between the compartments of the four-compartment aircraft

	$p_1 - p_2$	$p_3 - p_2$	$p_4 - p_1$	$p_4 - p_2$	$p_4 - p_3$
Differential pressure pick (kPa)	10.89	10.09	8.59	10.87	4.23

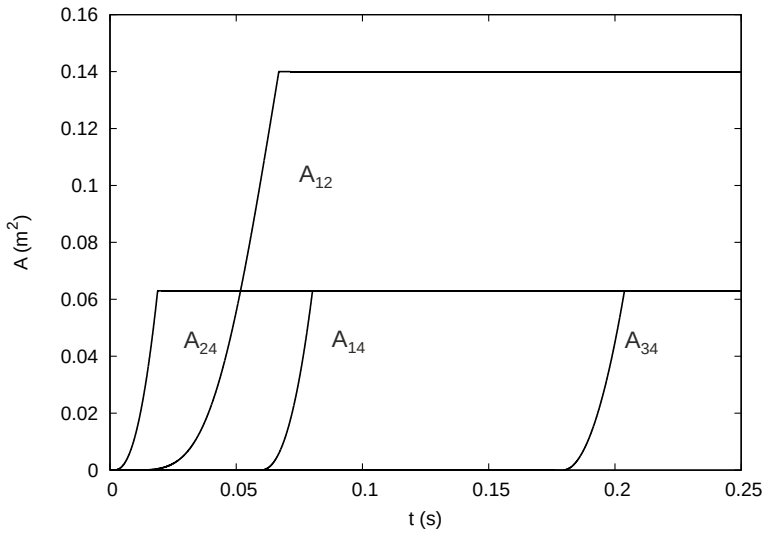

Fig. 15 Area variation of the active venting versus time; four-compartment aircraft

Table 4 Starting and total opening times of the blowout panels of the four-compartment aircraft

Compartments	1-2	1-4	2-4	3-4
Initial time to overcome the release pressure, t_0 (ms)	3.3	53.9	1.8	186.6
Opening time* (ms)	55.6	27.2	23.2	34

*Time for reaching the maximum venting area from t_0

compartments are experienced. Pressure picks are also given in a tabular form in Table 3. It should be noted that the maximum pressure loads are established at the interfaces cockpit/entryway and cargo/entryway, and they are experienced almost simultaneously.

Fig. 15 shows the opening of the active vents. The starting time and the opening durations of each blowout panel are also quoted in Table 4. In the first instants of the decompression, outflow to external ambient only interests entryway and passengers cabin from passive venting. After 1.8 ms, the translational panel between cargo and entryway activates, allowing for additional mass air participating in the analysis. At $t = 3.3$ ms, also the swinging door starts opening and cockpit air mass flows towards the damaged entryway. When the remaining blowout panels are activated, a complex air mass movement is verified within the fuselage.

6. Conclusions

An isentropic model for rapid and explosive decompression analyses has been developed in this work. Particular attention has been focused on the modeling of active venting system. A numerical procedure based on a direct integration scheme is also been provided for the resolution of the nonlinear system of ODEs resulting from the analysis of multi-compartment aircraft. The proposed model is used for (but not limited to) the analysis of pressurized aircraft, ranging from single- to four-compartment cabins. The validity of the present model is demonstrated through comparison with analytical and numerical solutions from the literature. The results highlight the importance of considering the opening dynamics of hinged and translational blowout panels. Assuming instantaneous opening results, in fact, into non-negligible underestimation of the pressure loads acting on structures.

References

Bréard, C., Lednicer, D., Lachendro, N. and Murvine, E. (2004), "A CFD analysis of sudden cockpit decompression", *42nd AIAA Aerospace Science Meeting and Exhibit*, AIAA Paper 2004-0054, Reno, USA, January.

Burlutskiy, E. (2012), "Numerical analysis on rapid decompression in conventional dry gases using one-dimensional mathematical modeling", *Int. Sci. Index*, **6**(3), 250-254.

Daidzic, N.E. and Simones, M.P. (2010), "Aircraft decompression with installed cockpit security door", *J. Aircraft*, **47**(2), 490-504.

Demetriades, S.T. (1954), "On the decompression of a punctured cabin in vacuum flight", *Jet Propulsion*, January-February.

European Aviation Safety Agency - EASA (2014), "Certification Specifications and Acceptable Means of Compliance for Large Aeroplanes, CS-25/Amendment 15".

Garner, R.P. (1999), "Concepts providing for physiological protection after cabin decompression in the altitude range of 60000 to 80000 feet above sea level", U.S. Department of Transportation, Rept. DOT/FAA/AM-99/4.

Haber, F. (1950), "Physical process of explosive decompression", *J. Aviat. Med.*, **21**(6), 495-499.

Haber, F. and Clamann, H.G. (1953), "Physics and engineering of rapid decompression: a general theory of rapid decompression", *U.S. Air Force School of Aviation Medicine*, Rept. 3, Randolph Field, Texas, USA.

Holman, J.P. (1980), *Thermodynamics*, McGraw-Hill, Singapore.

Langley, M. (1971), "Decompression of cabins", *Aircraf. Eng. Aerosp. Tech.*, **43**, 24-25.

Mavriplis, F. (1963), "Decompression of a pressurized cabin", *Can. Aeronaut. Space J.*, **9**(10), 313-318.

National Transportation Safety Board – NTSB (1989), "Aircraft accident report, Aloha Airlines, Flight 243, Boeing 737-200, N73711, near Maui, Hawaii, April 28, 1988", United States Government, Rept. NTSB/AAR-89/03.

Pratt, J.D. (2006), "Rapid decompression of pressurized aircraft fuselages", *J. Fail. Anal. Prevent.*, **6**(6), 70-74.

Roth, E.M. (1968), "Rapid (explosive) decompression emergencies in pressure-suited subjects", NASA Technical Report, Rept. CR-1223.

Streeter, V.L. and Wylie, E.B. (1975), *Fluid Mechanics*, McGraw-Hill, New York, NY, USA.